Development of CdZnTe pixel detectors for astrophysical applications

Fiona A. Harrison, Steven E. Boggs, Aleksey E. Bolotnikov, C. M. Hubert Chen, Walter R. Cook, et al.

Fiona A. Harrison, Steven E. Boggs, Aleksey E. Bolotnikov, C. M. Hubert Chen, Walter R. Cook, Steven M. Schindler, "Development of CdZnTe pixel detectors for astrophysical applications," Proc. SPIE 4141, Hard X-Ray, Gamma-Ray, and Neutron Detector Physics II, (21 November 2000); doi: 10.1117/12.407574

SPIE.

Event: International Symposium on Optical Science and Technology, 2000, San Diego, CA, United States

Invited Paper

Development of CdZnTe pixel detectors for astrophysical applications

F. A. Harrison, S. E. Boggs, A. Bolotnikov,
C. M. H. Chen, W. R. Cook, S. M. Schindler

Space Radiation Laboratory, 220-47
Division of Physics, Mathematics and Astronomy
Caltech, Pasadena, CA 91125

ABSTRACT

Over the last four years we have been developing imaging Cadmium Zinc Telluride pixel detectors optimized for astrophysical focusing hard X-ray telescopes. This application requires sensors with modest area ($\sim$ 2cm $\times$ 2 cm), relatively small ($\lesssim 500\mu$m) pixels and sub-keV energy resolution. For experiments operating in satellite orbits, low energy thresholds of $\sim 1-2$ keV are also desirable. In this paper we describe the desired detector performance characteristics, and report on the status of our development effort. In particular, we present results from a prototype sensor with a custom low-noise VLSI readout designed to achieve excellent spectral resolution and good imaging performance in the $2-100$ keV band.

1. INTRODUCTION

The recent development of depth-graded multilayer optics (e.g. Christensen *et al.* 2000) will enable large-area focusing telescopes to be employed in the hard X-ray band for the first time. Traditional metal-coated grazing-incidence X-ray mirrors of the type employed on the *Einstein, ASCA*, and *Chandra* satellites are limited to energies below $\sim$10 keV. This is due to the approximately linear decrease with energy of the incidence angle for which significant reflectance can be achieved. Very small incidence (or graze) angles result in small telescope fields of view and long focal lengths are required to achieve high throughput. Graded multilayer coatings, which operate on the principal of Bragg reflection, increase the maximum graze angles achievable at high energies, allowing practical systems with reasonable fields of view to be designed for energies up to $100-200$ keV.

The first use of focusing optics in this band will result in dramatic ($10-100$ fold) sensitivity improvements (see Fig. 1, enabling entirely new types of astrophysical investigations. Previous experiments have relied on indirect modulation schemes (simple collimators or coded apertures) for imaging and background subtraction. In this type of system, the experiment collecting area is approximately equivalent to or less than the detector area. This means that the background in each resolution element on the sky is equal to the entire detector background. Because typical background countrates are much larger than those of the average astronomical hard X-ray source, these instruments are limited in sensitivity, even for large (a few thousand cm^2) detector areas. In contrast, by using a concentrating telescope (collecting area much larger than detector area) to focus the signal onto a small spot on the detector, source-limited observations can be achieved, with greatly improved sensitivity. Furthermore, the sensors are compact, so that implementing high-performance systems is possible. In particular high spectral resolution sensors are costly, and generally not practical to deploy in experiments requiring large detector areas.

Several future astronomical instruments plan to incorporate focusing multilayer hard X-ray mirrors. At least two balloon payloads, the *High Energy Focusing Telescope (HEFT)*[2] and *InFocμs*,[3] will be launched in the next three years. In addition, the *Constellation X-ray Mission (Con-X)* plans to include a grazing-incidence system, the Hard X-ray Telescope (HXT),[4] to extend the mission's spectral coverage to E$\gtrsim$ 50 keV. This satellite experiment is included in NASA's Strategic Plan for a launch in the upcoming decade.

Our group at the Caltech Space Radiation Laboratory is currently developing CdZnTe focal plane sensors designed for two of these experiments: *HEFT* and the *Con-X* HXT. We are optimizing these detectors for spectral resolution,

Further author information: (Send correspondence to Fiona A. Harrison)
E-mail: fiona@srl.caltech.edu

Hard X-Ray, Gamma-Ray, and Neutron Detector Physics II, Ralph B. James, Richard C. Schirato, Editors,
Proceedings of SPIE Vol. 4141 (2000) © 2000 SPIE. · 0277-786X/00/$15.00

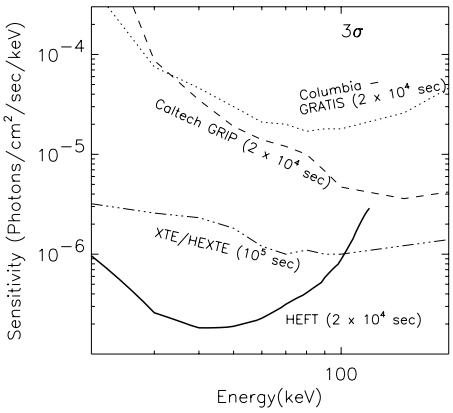

Figure 1. *The sensitivity of the* HEFT *experiment for observations from a balloon platform compared to the large-area coded aperture instruments* GRIP *and* GRATIS. *The energy bandwidth is $\Delta E/E = 50\%$, and we assume an atmospheric column depth of 3.5 g cm^{-2}. This demonstrates the large improvement in signal to noise possible with focusing experiments in this bandpass.*

imaging performance, and low-energy ($\sim$ 1 keV) threshold. In this paper we provide a brief description of the instruments' scientific goals, the required sensor performance, and the associated detector technical parameters. Section 4 describes the architecture of the sensors we are developing, and in Section 5 we present performance results to-date. Finally, we describe our plans for future effort.

2. SCIENTIFIC GOALS FOR FOCUSING HARD X-RAY TELESCOPES

The scientific programs for focusing hard X-ray telescopes emphasize the new capabilities made possible by this technology: high-sensitivity in some cases combined with good spectral resolution. Examples of specific scientific goals include broad-band studies of Active Galactic Nuclei (AGN), mapping of line emission from nuclear decays in young supernova remnants, and time-resolved spectroscopy of cyclotron resonance scattering features in high-magnetic field pulsars. We illustrate with a few specific examples below, emphasizing those which drive the instrument technical requirements.

Mapping ^{44}Ti in Young Supernova Remnants. Several key nuclear decay lines from elements synthesized in supernova explosions are observable in the hard X-ray band. Primary among these is ^{44}Ti, which decays to ^{44}Sc ($\tau = 87$ yr), producing dominant emission lines at 68 keV (91%) and 78 keV (97%). The daughter nucleus quickly decays to ^{44}Ca ($\tau = 5.4$ hours), producing a dominant emission line at 1157 keV (100%), which has been observed by the COMPTEL MeV experiment on the *Compton Gamma-ray Observatory*. ^{44}Ti is produced in core-collapse events in the region near the mass-cut (the boundary between material that is ejected and that which falls back onto the compact remnant of the explosion), and its distribution is therefore sensitive to the explosion mechanism and the ejecta dynamics.[5]

Producing maps of nearby remnants in our galaxy in ^{44}Ti is a high-priority observation for the *HEFT* balloon experiment. The instrument effective area will extend to $\sim$100 keV, and the detector development has emphasized high spectral resolution to map doppler broadening and shifts of the decay lines, providing further diagnostics of the explosion. The arcminute imaging to be achieved by the optics will allow mapping of this emission with sufficient resolution to observe features seen by X-ray instruments (Fig. 2).

Broadband observations of active galactic nuclei. Broadband ($0.5 - 50$ keV) X-ray spectral measurements of AGN provide powerful constraints on the physical conditions in the various emission regions and on the source geometry. In particular, measurements of the high-energy continuum ($E > 10$ keV) are critical in interpreting the line emission (from atomic transitions in highly-excited heavy elements) which dominates the low-energy spectrum. In some sources the continuum is in fact only visible above $\sim$10 keV, as it is absorbed by a dense "torus" of material surrounding the central emission region. Below 10 keV such sources are observable only in reprocessed (reflected) radiation.

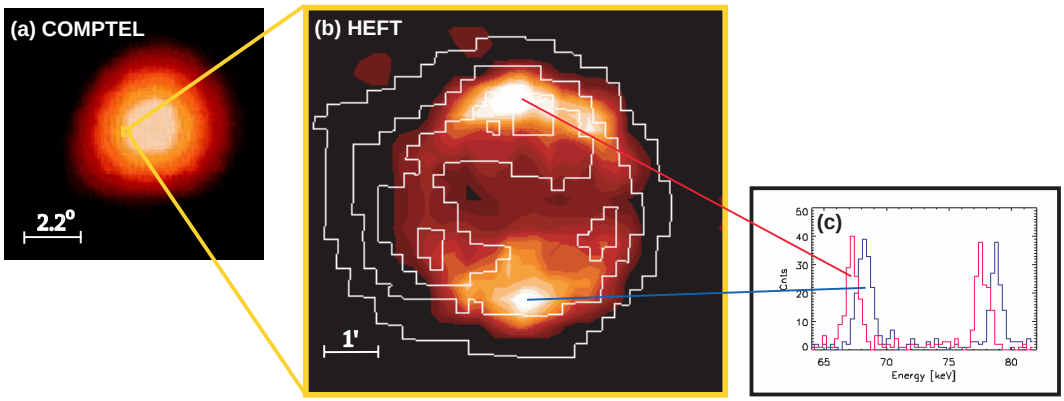

Figure 2. *Comparison of ^{44}Ti measurements from the Cas A SNR for the COMPTEL observation (1.157 MeV, 2.2° resolution)[left panel], and a simulation of a* HEFT *(68/78 keV, 1′resolution, 80 ksec) LDB observation [right panel]. The simulation assumes a (clearly resolved) clumpy, axisymmetric explosion. The ROSAT contour plot is shown for comparison. Also shown are the spectra of the two hemispheres, assuming that the top one was ejected away from the observer at -2000 km/s, and the bottom one toward the observer at +2000 km/s – moderate velocities for this SNR. Each hemisphere was also assumed to have an internal velocity dispersion of 1000 km/s.*

Broadband X-ray spectroscopy of AGN is a primary science driver for the *Constellation-X* mission. This experiment will incorporate a focusing hard X-ray telescope (HXT) to complement the large-area spectroscopy telescope which operates in the traditions $0.1 - 10$ keV band. The HXT is optimized for sensitive continuum measurements up to ∼50 keV over a few arcminute FOV.

Spectroscopic observations of cyclotron resonance scattering features in high magnetic field neutron stars. Cyclotron scattering resonance features (CSRFs) are formed as electrons accreting onto the surface of a highly magnetized neutron star undergo transitions between discrete Landau levels at the fundamental frequency, $E_c = 11.6\ keV \times (B/10^{12}\ G)$, and its harmonics. These transitions create absorption and emission line features in the emission spectrum, which can reveal much about the structure of the underlying neutron star and the accretion process. The line energy provides a direct measurement of the surface magnetic field strength, however much more information is contained in the CSRF shape. The line profiles reveal the spatial distribution of the field, the geometry of the accretion flow, and the plasma optical depth and temperature, which can be used to set limits on the luminosity and the distance of the source as well as the accretion rate (see e.g.[6]).

For typical magnetic field strengths, these lines fall lie between $\sim 10 - -70$ keV. Although many of these accreting sources are bright, resolving the line features as a function of pulse phase requires high-sensitivity observations.

3. FOCAL PLANE SENSOR PERFORMANCE REQUIREMENTS

Parameter	*HEFT*	*Con-X* HXT
energy band	$20 - 100$ keV	$< 5 - > 40$ keV ($1 - 60$ goal)
FOV	$10'$ (50 keV)	$\geq 8'$ ($6 - 40$ keV)
angular resolution	$1'$	$< 1'$ ($30''$ goal)
collecting area	200 cm^2 (50 keV)	1500 cm^2 (40 keV)
energy resolution (FWHM)	< 1 keV (68 keV)	< 1.2 keV (6 keV)

Table 1. *HEFT* and *Con-X* performance goals.

The scientific goals described above drive the desirable performance characteristics of future balloon and satellite-based experiments. Table 1 summarizes these for *HEFT* and *Con-X*. Both have worst-case angular resolution goals of 1 ′. The *HEFT* energy band extends from the atmospheric cutoff of ∼20 keV at the low end to 100 keV, in order to cover both ^{44}Ti lines. Because the *HEFT* scientific goals include spectroscopy of nuclear lines and CRSFs, the

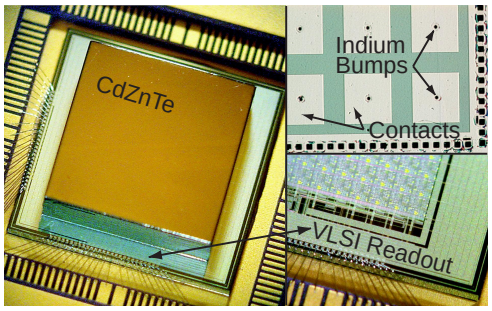

Figure 3. *Photo of the* HEFT *prototype, showing the detector geometry and packaging. In the final detector array, four CdZnTe will be tiled to fill the focal plane.*

spectral resolution goal is aggressive – better than 1 keV FWHM at the ^{44}Ti line energies. The *Con-X* HXT is emphasizing continuum observations at lower energy, and the resolution requirement is consequently less stringent.

Table 2 shows the telescope parameters for these two experiments, along with the sensor requirements associated with the performance goals for the telescopes as currently designed. Although the bandpass and spectral resolution requirements differ, both instruments require a very low level of electronic noise. For *HEFT* this is to achieve good spectral resolution, and for *Con-X* it allows a threshold at low X-ray energies. The detector and pixel dimensions are also similar, in spite of the different telescope focal lengths, due to the somewhat smaller FOV and more aggressive angular resolution goal of *Con-X*.

Parameter	*HEFT*	*Con-X* HXT
Telescope parameters		
focal length	6 m	10 m
optics	conical approx. Wolter I (14 modules)	Wolter I or approx. (12 modules)
Sensor requirements		
pixel size ($1/3 \times \Delta\theta \times f$	580μm	480 μm
energy band	20 – 100 keV	5 - 60 keV
energy resolution (FWHM)	$<$ 1 keV (68 keV)	$<$ 1.2 keV (6 keV)
dimensions (FOV $\times f$)	2.1 $\times$ 2.1 cm	2.3 $\times$ 2.3 cm
quantum efficiency	$>$ 90% (20 – 100 keV)	$>$ 90% (6 – 60 keV)
trigger required	yes	yes
maximum countrate	100 ct/s/pixel	100 ct/s/pixel
	500 ct/s/module	500 ct/s/module
typical countrate	few ct/s/module	few ct/s/module
time resolution	10μs	10 μs

Table 2. Telescope parameters and sensor requirements for *HEFT* and *Con-X*.

4. CDZNTE PIXEL DETECTOR DESIGN

We are developing CdZnTe pixel sensors and a custom low-noise VLSI readout designed to meet the *HEFT* and *Con-X* requirements described above. Fig. 3 shows the basic detector architecture. A CdZnTe sensor with the anode side segmented into contacts is indium bump bonded to the VLSI readout, where each pixel is connected to a separate readout chain. Each sensor element is 1.3 cm $\times$ 1.3 cm on a side (limited by the availability of large, uniform CdZnTe and the VLSI reticle size). To fill the focal plane, we will tile the sensors in a 4 $\times$ 4 array, minimizing the gap in between to the extent possible. Table 3 summarizes the characteristics of the *HEFT* flight detectors.

Pixel design. The goals in designing the CdZnTe pixel contacts are to minimize the size (and therefore the readout input capacitance), while at the same time avoiding significant charge loss for events occuring at the pixel

pixel size	500 μm	contact dimension	350 – 400 μm
hybrid size	1.3 × 1.3cm	typ bias	300 V
CdZnTe thickness	2 mm	typ grid–contact bias	12 V
operating temp.	-10 – -20°C	power/pixel	50μW

Table 3. HEFT sensor parameters.

edges. The latter occurs when charge reaches the low-field region occuring in the gap between pixel contacts, where it becomes trapped.[7] For a simple (two-terminal) detector, optimizing the overall performance involves trading the benefit of smaller contacts against the detriment of larger gaps.

The severity of the charge loss of course depends on the electric field geometry, which is determined not only by the contact and gap size, but also by the ratio of bulk to surface conductivity. The higher the surface conductance relative to the bulk, the greater the fraction of field lines that terminate in the gaps. If there is no electric field component parallel to the surface, the charge reaching the gap will not be directed toward the anode.

Because of the above effects, we are employing a three-terminal design for the pixel contact in order to minimize contact size yet avoid significant inter-pixel charge loss. We include thin strips between the square pixel contacts, held at a potential intermediate between the cathode and anode. This "grid" increases the electric field component on and parallel to the detector surface (see Bolotnikov *et al.* (2000) for details). Because we are not attempting to redirect the field lines to the anode entirely, we can operate with a modest grid – anode voltage (< 15V), so that the leakage current is minimal, and doesn't degrade the spectral resolution.

Readout architecture. We have developed a custom, low-noise CMOS readout for *HEFT* and *Con-X*. This device, designed at Caltech's Space Radiation Laboratory, has a separate readout chain for each pixel, where all pixel-specific cicuitry fits within a 450μm square. Each readout contains a charge-sensitive preamplifier and a pulse-sampling circuit. After an event, external logic reads a tag bit for each pixel, identifying those triggered. Sixteen analog samples of the waveform are then read for those pixels and their nearest neighbors for off-chip A/D conversion and digital filtering to extract the pulseheight.

5. PROTOTYPE PERFORMANCE

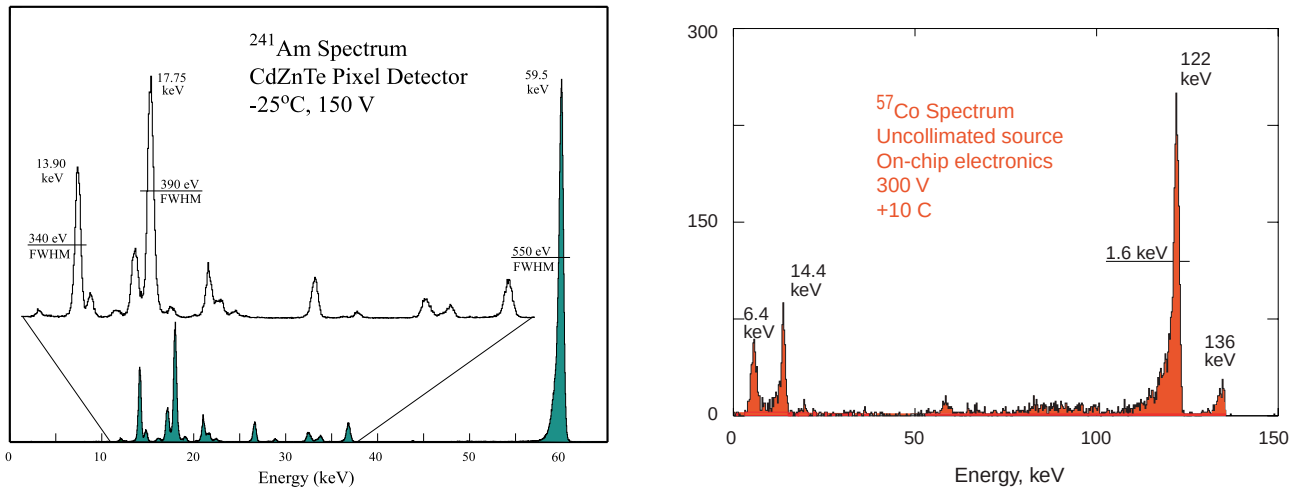

Figure 4. Left: Measured spectrum of a ^{241}Am source collimated to the center of a pixel of the *HEFT* detector prototype operated at -25 °C. The rms electronic noise contribution is 0.25 keV equivalent (50 e$^-$), and the threshold is set at ∼2 keV. Right: Measured ^{57}Co spectrum for an uncollimated source taken at 10°C.

We have developed and tested prototype 8 × 8 pixel sensors using a first-generation readout chip indium bump bonded to two- as well as three-contact CdZnTe sensors. The architecture of the peak detecting circuit in the first

prototype hybrids differs from that described above (see Cook *et al.* (1998)[9] for details), due to improvements made in the second-generation chip. These prototype devices have larger pixels ($650 \times 680\mu$m pitch) than we ultimately plan to use on *HEFT*.

The results obtained with these prototype hybrids demonstrate that the desired low-noise, high-resolution, and good imaging performance is achievable in a pixel architecture. Fig. 4 shows both an ^{241}Am (59/5 keV) and a ^{57}Co (122 keV) spectrum. The ^{241}Am (60 keV) was taken with the source collimated to a $\sim$200 μm spot in the center of the pixel, and the detector was cooled to -25 °C. Under these conditions the energy resolution is excellent: 550 eV FWHM at 59.5 keV, with only 50 e^- rms readout noise. The corresponding FWHM resolution measured at room temperature (18 °C) is 760 eV. The ^{57}Co spectrum was taken with the pixel fully illuminated at 10°C, and the measured resolution is 1.6 keV FWHM. We show results for multiple-pixel events (where charge is split between more than a single pixel), and measurements taken with three-terminal devices in Bolotnikov *et al.* (these proceedings).

6. FUTURE PLANS

Our development goal is to complete fabrication of our first flight sensors early in 2001. We have recently received our second-generation VLSI prototype chip from the foundry. This device has 8×8 450μm pitch pixels. We plan to couple this readout to CdZnTe sensors with a range of contact and gap sizes in order to pick the optimum geometry for the final hybrids. We expect to complete evaluation of the prototype hybrids in early Fall of this year. We are currently completing layout of the flight chip, which we expect to submit by the end of 2000.

7. CONCLUSION

The excellent resolution and low thresholds achieved with our prototype devices show that the *HEFT* and *Con-X* sensor performance goals can be achieved with CdZnTe pixel detectors. The material uniformity is sufficient to avoid severe imperfections for the sizes employed in these applications, the leakage current and electronic noise levels are low enough, and the charge trapping effects negligible enough that th sub-keV spectral resolution goal can be exceeded. Further work, however, remains to fully demonstrate the imaging performance (reconstruction of multiple-pixel events), and to show that dead area between hybrids can be maintained at an acceptable level.

8. ACKNOWLEDGEMENTS

This work is supported in part by NASA's SR&T program (NAGW 5-5289). FAH acknowledges support from a Presidential Early Career Award. We thank Jill Burnham and Branislav Kecman for their contributions to the detector bonding and VLSI development.

REFERENCES

1. F. E. Christensen, J. M. Chakan, W. W. Craig, C. J. Hailey, F. A. Harrison, V. Honkimaki, M. Jimenz-Garate, P. H. Mao, D. L. Windt, and E. Ziegler, "Measured reflectance of graded multilayer mirrors designed for astronomical hard x-ray telescopes," *Nuc.Inst.Meth.* **in press**, 2000.
2. F. A. Harrison, S. E. Boggs, A. Bolotnikov, F. E. Christensen, W. R. Cook, W. W. Craig, C. J. Hailey, M. Jimenez-Gerate, P. H. Mao, S. E. Schindler, and D. L. Windt, "Development of the high-energy focusing telescope (heft) balloon experiment." Proc. SPIE in press, 2000.
3. Y. Tawara, K. Yamashita, H. Kunieda, K. Tamura, A. Furuzawa, K. Haga, N. Nakajo, T. Okajima, H. Takata, P. J. Serlemitsos, J. Tueller, R. Petre, Y. Soong, K. Chan, G. S. Lodha, Y. Namba, and J. Yu, "Development of a multilayer supermirror for hard x-ray telescopes," *Proc. SPIE* **3444**, pp. 569–575, Nov. 1998.
4. F. A. Harrison, W. R. Cook, F. E. Christensen, O. Citterio, W. W. Craig, N. A. Gehrels, P. Gorenstein, J. E. Grindlay, C. J. Hailey, R. A. Kroeger, H. Kuneida, G. Pareschi, A. M. Parsons, R. Petre, and S. E. Romaine, "Technology development for the constellation-x hard-x-ray telescope," *Proc. SPIE* **3765**, pp. 104–111, Oct. 1999.
5. S. E. Woosley and T. A. Weaver *ApJS* **101**, p. 181, 1995.
6. P. Mszros and W. Nagel *ApJ* **298**, p. 147, 1985.
7. A. E. Bolotnikov, W. R. Cook, F. A. Harrison, A.-S. Wong, S. M. Schindler, and A. C. Eichelberger, "Charge loss between contacts of cdznte pixel detectors," *Nuc. Inst. Meth. A* **432**, p. 326, 1999.
8. A. E. Bolotnikov, S. E. Boggs, W. R. Cook, C. H. Chen, F. A. Harrison, and S. M. Schindler these proceedings, 2000.

9. W. R. Cook, J. A. Burnham, and F. A. Harrison, "Low-noise custom vlsi for cdznte pixel detectors," *Proc. SPIE* **3445**, pp. 347–354, Nov. 1998.